



Accurate Estimation of the Hurst Parameter of Long-Range Dependent Traffic Using Modified Allan and Hadamard Variances

Journal:	<i>IEEE Transactions on Communications</i>
Manuscript ID:	TCOM-06-0040.R1
Manuscript Type:	Transactions Paper Submissions
Date Submitted by the Author:	n/a
Complete List of Authors:	Bregni, Stefano; Politecnico di Milano, Dept. of Electronics and Information Jmoda, Luca; Politecnico di Milano, Dept. of Electronics and Information
Keyword:	Communication system traffic, Wavelet transforms, Time domain analysis, Internet, Fractals



Review

Accurate Estimation of the Hurst Parameter of Long-Range Dependent Traffic Using Modified Allan and Hadamard Variances

Stefano Bregni*, *Senior Member, IEEE*,
Luca Jmoda

Politecnico di Milano, Dept. of Electronics and Information
Piazza Leonardo Da Vinci 32, 20133 Milano, Italy.
Tel.: +39-02-2399.3503. Fax: +39-02-2399.3413
E-mail: bregni@elet.polimi.it (*managing author)

Index terms:

Communication system traffic, fractals, fractional noise, Internet, long-range dependence, self-similarity, time domain analysis, wavelet transforms.

ABSTRACT

Internet traffic exhibits self-similarity and long-range dependence (LRD) on various time scales. In this paper, we propose to use the Modified Allan Variance (MAVAR) and a Modified Hadamard Variance (MHVAR) to estimate the Hurst parameter H of LRD traffic series or, more generally, the exponent α of data with f^α ($\alpha < 0$) power-law spectrum. MHVAR generalizes the principle of MAVAR, a time-domain quantity widely used for frequency stability characterization, to higher-order differences of input data. In our knowledge, this MHVAR has been mentioned in literature only few times and with little detail so far.

The behaviour of MAVAR and MHVAR with power-law random processes and some common deterministic signals (viz. drifts, sine waves, steps) is studied by analysis and simulation. The MAVAR and MHVAR accuracy in estimating H is evaluated and compared to that of wavelet Logscale Diagram (LD). Extensive simulations show that MAVAR and MHVAR achieve significantly better confidence and no bias in H estimation. Moreover, MAVAR and MHVAR feature a number of other advantages, which make them valuable to complement other established techniques such as LD. Finally, MHVAR and LD are also applied to a real IP traffic trace.

Note

Part of this paper is based on "Improved Estimation of the Hurst Parameter of Long-Range Dependent Traffic Using the Modified Hadamard Variance", by S. Bregni and L. Jmoda, appeared in *Proc. of IEEE ICC 2006*, Istanbul, Turkey, June 2006.

Work partially funded by Ministero dell'Istruzione, dell'Università e della Ricerca (MIUR), Italy, under PRIN project MIMOSA.

I. INTRODUCTION

Internet traffic exhibits intriguing temporal correlation properties, such as self-similarity and long memory (long-range dependence) on various time scales [1]–[4]. Contrary to the classical Poisson assumption, these properties emphasize long-range time-correlation between packet arrivals. Fractional noise and fractional Brownian motion models are often used to describe such behaviour of Internet traffic series, which include, but are not limited to, cumulative or incremental data count transmitted over time, inter-arrival time series of successive TCP connections or IP packets, etc.

In a self-similar random process, a dilated portion of a realization (sample path) has the same statistical characterization than the whole. “Dilating” is applied on both amplitude and time axes of the sample path, according to a scaling parameter H called Hurst parameter. On the other hand, long-range dependence (LRD) is a long-memory property observed on large time scales, usually equated with an asymptotic power-law decrease of the power spectral density (PSD) $\sim f^{-\gamma}$ or, equivalently, of the autocovariance function. Under some hypotheses, the integral of a LRD process is self-similar (e.g., fractional Brownian motion, integral of fractional Gaussian noise).

In literature, a well-studied topic is the estimation of parameters that characterize self-similar and LRD random processes, aiming for example at best modelling traffic to the purpose of network simulation. Several algorithms exist, in particular, to estimate the parameters H and γ . To this aim, prominent attention has been given to methods based on wavelets [1]–[9].

In a different context, the Modified Allan Variance (MAVAR) is a well known time-domain quantity, originally proposed in 1981 for frequency stability characterization of precision oscillators [10]–[14], purposely designed to discriminate noise types with power-law spectrum, recognized very commonly in frequency sources. Moreover, telecommunications standards (ANSI, ETSI, ITU-T) specify some network synchronization requirements in terms of Time Variance (TVAR), closely related to MAVAR [15].

In paper [16], MAVAR was proposed for the first time as traffic analysis tool, to estimate parameters H and γ of LRD traffic series, pointing out its superior estimation accuracy and spectral

sensitivity. MAVAR was successfully applied to real network traffic analysis, allowing to identify fractional noise in measurement data [16]—[18].

In this paper, we refine and extend the scope of research [16], investigating further the properties of MAVAR as well as of some other time-domain variances, with the aim at improving the estimation accuracy of H and γ . MAVAR and a Modified Hadamard Variance (MHVAR) are studied by analysis and simulation. In our knowledge, this particular Hadamard variance has been mentioned in literature only few times and has not been treated in detail so far. Then, methods based on MAVAR and MHVAR to estimate the Hurst parameter and, more generally, to identify fractional noise components in traffic data are proposed.

Extensive simulations show that MAVAR and MHVAR achieve the highest confidence with no bias in H and γ estimation. Both methods have been evaluated on thousands of pseudo-random LRD data series and compared to the well-established logscale diagram (LD) technique based on wavelet analysis [3][8]. Moreover, the behaviour of MAVAR and MHVAR on some deterministic signals (viz. drifts, steps and periodic components), common examples of nonstationarity in data under analysis, is studied. Finally, a real IP traffic trace is also analyzed, providing a sound example of application.

II. SELF-SIMILARITY AND LONG-RANGE DEPENDENCE

A random process $X(t)$ (say, cumulative packet arrivals in time interval $[0, t]$), is said to be *self-similar*, with scaling parameter of self-similarity or Hurst parameter $H > 0$, $H \in \mathfrak{R}$, if

$$X(t) \stackrel{d}{=} a^{-H} X(at) \quad (1)$$

for all $a > 0$, where $\stackrel{d}{=}$ denotes equality for all finite-dimensional distributions [1][2][3][19]. In other terms, the statistical description of $X(t)$ does not change by *scaling* simultaneously its amplitude by a^{-H} and the time axis by a .

In practice, the class of self-similar (H-SS) processes is usually restricted to that of *self-similar processes with stationary increments* (or H-SSSI processes), which are “integral” of some stationary process. For example, consider the δ -increment process of $X(t)$, defined as $Y_\delta(t) = X(t) - X(t - \delta)$ (say, packet arrivals in the last δ time units). For a H-SSSI process $X(t)$, $Y_\delta(t)$ is stationary and $0 < H < 1$ [2][3][19].

Long-range dependence (LRD) of a process is defined by an asymptotic power-law decrease of its autocovariance or equivalently PSD functions [1][2][3]. Let $Y(t)$ be a second-order stationary stochastic process. The process $Y(t)$ exhibits LRD if its autocovariance function follows asymptotically

$$R_Y(\delta) \sim c_1 |\delta|^{\gamma-1} \quad \text{for } \delta \rightarrow +\infty, 0 < \gamma < 1 \quad (2)$$

or, equivalently, its power spectral density (PSD) follows asymptotically

$$S_Y(f) \sim c_2 |f|^{-\gamma} \quad \text{for } f \rightarrow 0, 0 < \gamma < 1 \quad (3).$$

In general, a random process with non-integer power-law PSD is also known as fractional (not necessarily Gaussian) noise. It can be proven [2][3] that H-SSSI processes $X(t)$ with $1/2 < H < 1$ have long-range dependent increments $Y(t)$, with

$$\gamma = 2H - 1 \quad (4).$$

Strictly speaking, the Hurst parameter characterizes self-similar processes, but it is frequently used to label also the LRD increments of H-SSSI processes. In this paper, we follow this common custom with no ambiguity. Hence, the expression ‘‘Hurst parameter of a LRD process’’ (characterized by parameter γ) denotes actually, by extension, the Hurst parameter $H = (\gamma+1)/2$ of its integral H-SSSI parent process.

By definition, LRD consists in a power-law behaviour of certain second-order statistics versus the duration τ of the observation interval. Therefore, several techniques exist to estimate H and γ of data series supposed self-similar or LRD, both in the time domain (e.g., variance-time plot) and in the frequency domain (e.g., periodogram) [1][3][6], which are based on measuring the slope of a linear fit in a log-log plot. A class of more advanced techniques is based on wavelet analysis [3][5][7]–[9]. Among wavelet-based techniques, the so-called *logscale diagram* (LD) is of utmost importance [3][8]. It analyzes data over an interval of time scales (octaves), ranging from 1 (finest detail) to a longest scale given by data finite length. Also in this case, by observing the diagram slope, H and γ are estimated.

III. THE MODIFIED ALLAN VARIANCE

This section introduces MAVAR and briefly summarizes basic properties most relevant to our aim. The interested reader is referred to the bibliography for all details.

A. Background and a Wider Perspective

In stability characterization of precision oscillators, PSD power-law models (3) are common for phase and frequency noise, with integer values $0 \leq \gamma \leq 4$ found in experimental results (e.g., the phase deviation follows a random walk, when the instantaneous frequency is affected by white noise). Although values $\gamma \geq 1$ yield model pathologies, such as infinite power (variance) and even nonstationarity¹, this model is widely used, considering also that real-world constraints imply measurement finite bandwidth and duration. For an excellent survey on characterization of frequency stability in precision oscillators, read Rutman [21].

To circumvent such pathologies, in particular the variance increasing indefinitely with data length if $\gamma \geq 1$, a useful approach is evaluating the variance of the M -th derivative (supposed stationary) of the process (in wavelet analysis, this is equivalent to increasing the number of vanishing moments). In particular, the Allan Variance (AVAR), recommended by IEEE in 1971 [22] for characterization of frequency stability after D. W. Allan [23], is a kind of variance of the second difference of phase samples. The structure function theory, developed by Lindsey and Chie [24], gives a unifying view of time-domain quantities evaluated more generally on the M -th difference (supposed stationary) of data. To probe further, see also [14] and [25]—[28].

In the different context of statistical inference, the estimation of parameters of fractional Brownian motions by the K -th moments of their discrete variations was studied in [29][30], covering theoretical aspects as robustness of estimators and convergence theorems. Although not mentioned explicitly, Allan and related variances may be set also in this more general framework.

Abry and Veitch, in their fundamental paper [8] proposing the wavelet LD, did mention the AVAR and noticed that its definition can be rephrased in terms of the Haar wavelet. Under this perspective, the second difference in AVAR definition corresponds to the two vanishing moments of this wavelet. Several properties of Allan and related variances may be derived also via the wavelet formalism. However, while these Authors recognized fine qualities of AVAR for H estimation, they did not investigate it further, since their method based on Daubechies wavelets outperforms it.

A substantial improvement of AVAR is the Modified Allan Variance, which has played a prominent role in stability characterization of precision oscillators since 1981 [10]–[15]. Being based on data second difference, as AVAR, it converges to finite values for all power-law noise types with $\gamma < 5$ and is insensitive to data linear drift. Nevertheless, it allows more accurate estimation of the parameter γ , over the full range $0 \leq \gamma < 5$ and in particular for $0 \leq \gamma \leq 1$, where AVAR exhibits poor discrimination capability. These properties suggest its fruitful application also to LRD and self-similar traffic analysis and call for a thorough investigation on its usefulness in this field.

B. Definition and Estimator in the Time Domain

Given an infinite sequence $\{x_k\}$ of samples of $x(t)$ with sampling period τ_0 , MAVAR is defined as

$$\begin{aligned} \text{Mod } \sigma_y^2(\tau) &= \frac{1}{2n^2\tau_0^2} \left\langle \left[\frac{1}{n} \sum_{j=1}^n (x_{j+2n} - 2x_{j+n} + x_j) \right]^2 \right\rangle = \\ &= \frac{1}{2} \left\langle \left[\frac{1}{n} \sum_{j=1}^n (y_{j+n} - y_j) \right]^2 \right\rangle \end{aligned} \quad (5)$$

where $\langle \cdot \rangle$ denotes infinite-time averaging, $\tau = n\tau_0$ is the observation interval and y_k is the average value of $y(t) = x'(t)$ over interval τ beginning at t_k , i.e. the k -th sample of the first difference of $\{x_k\}$ with lag τ :

$$y_k(\tau) = \frac{1}{\tau} \int_{t_k}^{t_k+\tau} y(t) dt = \frac{x_{k+n} - x_k}{n\tau_0} \quad (6).$$

Thus, MAVAR is a kind of variance of the first difference of $\{y_k\}$ or of the second difference of $\{x_k\}$ (note: differences multiplied by τ). In very brief, it differs from the unmodified Allan variance in the additional internal average over n adjacent samples: for $n = 1$ ($\tau = \tau_0$), the two variances coincide.

In practice, given a finite set of N samples $\{x_k\}$, spaced by τ_0 , an estimate of MAVAR can be computed using the ITU-T standard estimator [14][15]

$$\text{Mod } \sigma_y^2(n\tau_0) = \frac{1}{2n^4\tau_0^2(N-3n+1)} \sum_{j=1}^{N-3n+1} \left[\sum_{i=j}^{n+j-1} (x_{i+2n} - 2x_{i+n} + x_i) \right]^2 \quad (7)$$

¹ In fractional Brownian motion, defining the precise meaning of “power spectral density”, proportional to $|f|^{-\gamma}$ with $\gamma \geq 2$, raises some conceptual concern due to nonstationarity of these processes. See [20] for a discussion and clarification.

with $n = 1, 2, \dots, \lfloor N/3 \rfloor$. A recursive algorithm for fast computation of this estimator exists [14], which cuts down the complexity of evaluating MAVAR for *all* $\lfloor N/3 \rfloor$ values of n to $O(N^2)$ instead of $O(N^3)$.

The point estimate (7), computed by averaging $N-3n+1$ terms, is a random variable itself. Exact computation of confidence intervals is not immediate and, annoyingly enough, depends on the spectrum of the underlying noise [31]—[37]. However, in general, confidence intervals are negligible at short τ and widen for longer τ , where fewer terms are averaged. Interval width is approximately proportional to $m^{-1/2}$, with m equal to the number of averaged terms. In practice, being N usually in the order of 10^4 and above, $\text{Mod } \sigma_y^2(\tau)$ exhibits random ripple due to poor confidence only at the right end of the curve.

C. Equivalent Definition in the Frequency Domain

As for other variances [21][38], the MAVAR time-domain definition can be translated to an equivalent expression in the frequency domain, allowing a more profound understanding of the behaviour of this quantity [13][14]. In fact, (5) can be rewritten as the mean square value of the output of a linear filter with impulse response $h_{\text{MA}}(n, t)$ properly shaped, i.e.

$$\text{Mod } \sigma_y^2(\tau) = \left\langle \left[\int_{-\infty}^{\infty} y(\xi) h_{\text{MA}}(n, t - \xi) d\xi \right]^2 \right\rangle \quad (8).$$

The filter impulse response $h_{\text{MA}}(n, t)$ is plotted in Fig. 1 for $n=6$ [14].

Hence, MAVAR can be equivalently defined in the frequency domain as

$$\text{Mod } \sigma_y^2(\tau) = \int_0^{\infty} S_y(f) |H_{\text{MA}}(n, f)|^2 df = \int_0^{\infty} S_y(f) \frac{2 \sin^6 \pi f \tau}{(n \pi f)^2 \sin^2 \pi \frac{\tau}{n} f} df \quad (9)$$

where $S_y(f) = S_x(f) \cdot (2\pi f)^2$ is the one-sided PSD of $y(t) = x'(t)$ and $H_{\text{MA}}(n, f)$ is the filter transfer function.

The square magnitude $|H_{\text{MA}}(n, f)|^2$, plotted in Fig. 2 for some values of the parameter n and having normalized f to $1/\tau$, takes the asymptotic expression, for $n \rightarrow \infty$ and keeping constant $n \tau_0 = \tau$:

$$\lim_{\substack{n \rightarrow \infty \\ n \tau_0 = \tau}} |H_{\text{MA}}(n, f)|^2 = 2 \frac{\sin^6 \pi f \tau}{(\pi f \tau)^4} \quad (10).$$

From Fig. 2, it can be seen that this limit is approached quickly for fairly low values of n ($n > 4$).

This transfer function is pass-band, with a narrow main lobe at $f \cong 0.4/\tau$. Hence, MAVAR allows

high-resolution spectral analysis by computation over τ . Analogously to the wavelet LD, H and γ of LRD data can be estimated by observing the $\text{Mod } \sigma_y^2(\tau)$ curve slope in a log-log plot.

D. Going Further and Beyond

After [16], we extended our scope of research to other time-domain variances, seeking even higher spectral resolution and better accuracy of estimation of H and γ . This section overviews the most interesting variances considered in our study, by analysis and simulation not reported here for conciseness.

Total Variance (TOTVAR) and *Modified Total Variance* are improvements of conventional estimators of AVAR and MAVAR [39]–[42]. Total estimators improve confidence for largest observation intervals τ , where few samples are averaged, by periodically extending the input data sequence beyond its finite length. Unfortunately, total estimators suffer bias, depending on τ and the type of underlying noise, which affects the curve slope in log-log diagrams. In practice, taking this bias into account makes cumbersome to estimate H and γ from total variance slope.

The *Hadamard Variance* (HVAR) was proposed by Baugh [43] in 1971 for high-resolution spectral analysis. Generally based on a linear combination of $M+1$ consecutive samples, HVAR may attain highest spectral selectivity, by adjusting appropriately the dead time between measurements and the weights of the $M+1$ samples [21]. In particular, the most useful definition of HVAR is based on weighting the $M+1$ samples with binomial coefficients (BC). This way, better spectral selectivity than AVAR is achieved [43][44]. The $(M+1)$ -samples BC-weighted HVAR is a variance of the M^{th} difference of input data, whereas AVAR is a 2nd-difference variance, i.e. based on 3 samples (cf. Sec. III.A).

A *Total Hadamard Variance* (TOTHVAR) has been defined too [44][45]. As other total variances, this estimator improves confidence for largest observation intervals τ , but suffers bias that makes cumbersome to estimate H and γ in practice.

In spite of its highest spectral resolution, HVAR is not able to discriminate effectively white ($\gamma=0$) from flicker ($\gamma=1$) noise, similarly to AVAR. This makes plain HVAR not suitable to our aim. Therefore, a *Modified Hadamard Variance* (MHVAR) is proposed and studied in this paper. MHVAR

has been derived by modifying the definition of the BC-weighted HVAR analogously to MAVAR. In our knowledge, such a modified HVAR has been mentioned in literature only few times (a.k.a. "pulsar variance") and expounded with little detail so far [36][46].

IV. THE MODIFIED HADAMARD VARIANCE

MHVAR generalizes the principle of MAVAR to higher-order differences of input data. Most formulas in this section are generalizations of MAVAR formulas.

A. Definition and Estimator in the Time Domain

Given an infinite sequence of samples $\{x_k\}$ with sampling period τ_0 , the MHVAR of order M (MHVAR- M) is defined as

$$\text{Mod } \sigma_{H,M}^2(\tau) = \frac{1}{M! n^2 \tau_0^2} \left\langle \left[\frac{1}{n} \sum_{j=1}^n \sum_{k=0}^M \binom{M}{k} (-1)^k x_{j+kn} \right]^2 \right\rangle \quad (11).$$

In brief, unmodified HVAR of order M is a kind of variance of the M^{th} difference of input data (but note the division by τ^2 instead of τ^{2M}). As MAVAR with AVAR, MHVAR differs from HVAR in the additional internal average over n adjacent samples: for $n=1$ ($\tau=\tau_0$), the two variances coincide. Moreover, note that, for $M=2$, MHVAR coincides with MAVAR. HVAR and MHVAR of order $M=3$ have been mostly considered in literature [21][36][43]—[46].

In practice, given a finite set of N samples $\{x_k\}$, again spaced by τ_0 , MHVAR can be estimated as

$$\text{Mod } \sigma_{H,M}^2(\tau) = \frac{\sum_{i=1}^{N-(M+1)n+1} \left[\sum_{j=i}^{i+n-1} \sum_{k=0}^M \binom{M}{k} (-1)^k x_{j+kn} \right]^2}{M! n^4 \tau_0^2 [N - (M+1)n + 1]} \quad (12)$$

with $n = 1, 2, \dots, \lfloor N/(M+1) \rfloor$. For $M=2$, estimator (12) coincides with (7).

As for MAVAR, exact computation of confidence intervals is not immediate and depends on the spectrum of the underlying noise [31][35]—[37][44]. However, in practice, being N usually in the order of 10^4 and above, $\text{Mod } \sigma_{H,M}^2(\tau)$ exhibits random ripple due to poor confidence only for largest τ .

B. Equivalent Definition in the Frequency Domain

Analogously to MAVAR (8)(9), MHVAR can be equivalently defined in the frequency domain. The square magnitude of the equivalent filter transfer function $H_{MH}(M, n, f)$ takes the asymptotic expression, for $n \rightarrow \infty$ and keeping constant $n\tau_0 = \tau$ (cf. eq. (10)):

$$\lim_{\substack{n \rightarrow \infty \\ n\tau_0 = \tau}} |H_{MH}(M, n, f)|^2 = \frac{2^{2(M-1)}}{M!} \left(\frac{\sin \pi f \tau}{\pi f \tau} \right)^4 (\sin \pi f \tau)^{2(M-1)} \quad (13).$$

As for MAVAR ($M=2$, Fig. 2), this limit is approached quickly for fairly low values of n (few units). Its square magnitude is plotted in Fig. 3 for some values of the parameter M , having omitted the constant factor $2^{2(M-1)}/M!$ and normalized f to $1/\tau$. All these transfer functions are pass-band, with a narrow main lobe at $f \cong 0.4/\tau \div 0.5/\tau$, which becomes narrower by increasing M .

V. BEHAVIOUR OF MAVAR AND MHVAR

In this section, the behaviour of MAVAR and MHVAR- M is studied with power-law random signals, drifts, periodic components and steps. Although MAVAR is a particular case of MHVAR- M ($M=2$), we will mention the two quantities explicitly, for clearness and according to tradition.

A. Power-Law Random Signals

It is convenient to generalize the LRD power-law model of spectral density (3). As customary in characterization of phase and frequency noise of precision oscillators [13][14][21][34], we deal with random processes $x(t)$ with one-sided PSD modelled as

$$S_x(f) = \begin{cases} \sum_{i=1}^P h_{\alpha_i} f^{\alpha_i} & 0 < f \leq f_h \\ 0 & f > f_h \end{cases} \quad (14)$$

where P is the number of noise types considered in the model, α_i and h_{α_i} are parameters ($\alpha_i, h_{\alpha_i} \in \mathfrak{R}$) and f_h is the upper cut-off frequency. Such random processes are commonly referred to as *power-law noise* or *fractional noise*. Note that $x(t)$ is not necessarily assumed Gaussian in this model.

Power-law noise with $-4 \leq \alpha_i \leq 0$ has been revealed in practical measurements of various physical phenomena (see again note), including phase noise of precision oscillators [14][22][21][34] and Internet

traffic [1][16][17], whereas P should be not greater than few units for the model being meaningful. If the process $x(t)$ is simple LRD (3), then $P=1$ and $-1 < \alpha_i < 0$. Finally, the case $\alpha_i > 0$ is less interesting and will be not considered in this work [3].

Under this general hypothesis, first we notice that, since $|H_{MH}(M, n, f)|^2$ behaves as $\sim f^{2(M-1)}$ for $f \rightarrow 0$, MHVAR- M convergence is ensured for $\alpha_i > -1-2M$, while MAVAR converges for $\alpha_i > -5$. Then, by considering separately each term of the sum in (14) and letting $P=1$, $\alpha = \alpha_i$, evaluation of frequency-domain definitions with (10) and (13) yields corresponding time-domain expressions $\text{Mod } \sigma_{H,M}^2(\tau)$ and $\text{Mod } \sigma_y^2(\tau)$. Complete formulas for MAVAR are available in [13][14]. Moreover, Rutman [21] presents a detailed overview about recognizing power-law random noise and polynomial drifts in time-domain measures, including unmodified Allan and Hadamard variances.

In summary, under the power-law PSD model (14) ($P=1$) and in the whole range of convergence $-1-2M < \alpha \leq 0$, both MAVAR and MHVAR- M are found to obey the simple power law (ideally asymptotically for $n \rightarrow \infty$, $n\tau_0 = \tau$, but in practice for $n > 4$)

$$\text{Mod } \sigma_{H,M}^2(\tau) \sim A_\mu \tau^\mu, \quad \mu = -3 - \alpha \quad (15)$$

If $P > 1$, it is immediate to generalize (15) to summation of powers $\sum_i A_{\mu_i} \tau^{\mu_i}$.

This is a fundamental result. If $x(t)$ obeys (14) and assuming sufficient separation between components, a log-log plot of $\text{Mod } \sigma_{H,M}^2(\tau)$ looks ideally as a broken line made of P straight segments (corresponding to the piecewise linear trend of the $S_x(f)$ log-log plot), whose slopes μ_i yield the estimates $\alpha_i = -3 - \mu_i$ of the fractional noise components dominant in different ranges of observation interval τ .

The logscale diagram [3][8] exhibits analogous behaviour. Actually, plots of $\log(\text{MAVAR}/\text{MHVAR})$ versus $\log(\tau)$ can be also seen as particular logscale diagrams, since modified Allan and Hadamard variances can be redefined in terms of appropriate wavelets too. In [3], logscale diagrams displaying two regions with different average slopes are referred to as *biscaling* phenomenon.

B. Deterministic Signals

It is of utmost interest to understand the behaviour of MAVAR and MHVAR also when $x(t)$

includes deterministic components, which are major examples of nonstationarity in Internet traffic.

1) **Offset and polynomial drift.** Let $x(t) = \sum_{j=0}^M C_j t^j$. By substitution in (11), we get that MHVAR- M (based on the M -th difference of input data) cancels data polynomial drift of order $<M$, but reveals a $\sim t^M$ drift, then assuming trend $\sim \tau^{2M-2}$. The MAVAR behaviour is obtained for $M=2$. Using wavelet formalism, this is explained by the fact that the MHVAR- M wavelet has M vanishing moments (cf. [8] Sec. III.B).

2) **Periodic Signals.** Let $y(t) = x'(t) = A \sin 2\pi f_m t$, with $S_y(f) = (A^2/2) \cdot \delta(f-f_m)$. Then, by substitution in the frequency-domain definition, we get (for $n \rightarrow \infty$, $n\tau_0 = \tau$):

$$\text{Mod } \sigma_{H,M}^2(\tau) = A^2 \frac{2^{2(M-1)-1}}{M!} \left(\frac{\sin \pi f_m \tau}{\pi f_m \tau} \right)^4 (\sin \pi f_m \tau)^{2(M-1)} \quad (16).$$

The MAVAR expression is obtained for $M=2$. Hence, MAVAR and MHVAR ripple with period $2/f_m$. (cf. [8] Sec. III.B.3)

3) **Steps.** Sudden changes of the average bit rate are not rare in Internet traffic, due for instance to traffic rerouting or link capacity adjustment. Let $x(t) = Au(t)$ (with $u(t) = 0$ for $t < 0$ and $u(t) = 1$ for $t \geq 0$). Since $y(t) = x'(t) = A\delta(t)$, from (8) we get

$$\text{Mod } \sigma_y^2(\tau) = \left\langle [A \cdot h_{MA}(n, t)]^2 \right\rangle = 0 \quad (17).$$

Thus, steps in $x(t)$ ideally do not affect MAVAR. In practice, the estimate (7) is computed on a finite interval $T = (N-1)\tau_0$ and is thus dependent on both τ and T . Even so, by numerous simulations (Sec. VII.B), we found that MAVAR and MHVAR are significantly affected only if the step size is very high, provided that T is reasonably long. Anyway, MHVAR- M slope (M even) is affected less than LD.

VI. USING MAVAR AND MHVAR FOR ESTIMATING THE HURST PARAMETER

Let us consider a LRD process $x(t)$ with PSD (3) and Hurst parameter $1/2 < H < 1$. Then, from (4) and (15), MAVAR and MHVAR- M follow $\sim \tau^\mu$ (ideally for $n \rightarrow \infty$) with $\mu = 2H-4$. In brief, the following procedure is suggested to estimate H :

1) compute MAVAR by (7) or MHVAR- M by (12), based on $\{x_k\}$, for integer values $1 \leq n < N/(M+1)$

- (we use a geometric progression of ratio 1.1, i.e. 24 values/decade, for finest rendering of trend);
- 2) by least-square linear regression, estimate the average slope μ of MAVAR/MHVAR in a log-log plot for $n > 4$ and excluding highest values of n , where confidence is lowest;
 - 3) if $-3 < \mu < -2$ (i.e., $-1 < \alpha < 0$, $0 < \gamma < 1$), get the estimate of the Hurst parameter as

$$H = \mu/2 + 2 \quad (18).$$

Under the more general hypothesis of power-law PSD (14), then up to P slopes μ_i can be identified ($-3 \leq \mu_i < 2M-2$) to yield the estimates $\alpha_i = -3 - \mu_i$ ($-1-2M < \alpha_i \leq 0$) of the P components of f^{α_i} noise.

Some care should be exercised against non-stationary terms in data analyzed (e.g., big steps, slow trends), which cause slope changes that may be erroneously ascribed to random power-law noise. On the other hand, polynomial drifts are cancelled, unless their order is greater than M . Thus, the order M can be conveniently adjusted. In [8] (Sec. III.B.4), similarly, it is suggested to increase the number of vanishing moments until the H estimate converges to a stable value, thus indicating that all smooth trends have been cancelled.

A key issue is to determine the confidence of these estimates and whether they are unbiased or not. In [8] (Sec. III.C), this problem is studied for the H estimator based on wavelet decomposition. Provided that the number of the vanishing moments is chosen appropriately, the estimator is proven to be unbiased (or with low bias on finite data sets). Closed forms of the variance and confidence intervals of this estimator are derived as well, although under a number of simplifying assumptions. Since MAVAR and MHVAR can be rephrased in terms of appropriate wavelets, it can be argued that similar results may be valid also for the estimator proposed herein.

Nevertheless, deriving exact expressions for the confidence intervals of H and α_i estimates is not immediate. Exact computation of confidence intervals of MAVAR and MHVAR estimates is tedious and even depends on the spectrum of the underlying noise (Secs. III.B, IV.A). Therefore, the evaluation of confidence intervals of estimates of H and α_i results even more complex, depending also on the algorithm used to estimate the average slope of curves and on the interval on which this is carried out. Being analysis cumbersome, we chose to evaluate empirically the accuracy of the method proposed, by simulation on pseudorandom data, as done for example in [6].

VII. SIMULATION RESULTS

The accuracy of the MAVAR/MHVAR method was evaluated by extensive simulations, by comparison to the well-established wavelet LD technique [3][8]. All LD results were computed running standard scripts [47], using Daubechies wavelet with $N_v=3$ vanishing moments (LD-3).

A. Accuracy Evaluation

The MHVAR-3, MAVAR and LD-3 methods were applied to LRD pseudo-random data series $\{x_k\}$ of length N , generated with one-sided PSD $S_x(f) = hf^\alpha$ ($-1 < \alpha \leq 0$) for assigned values of $H = (1-\alpha)/2$. The generation algorithm is by Paxson [48]: a vector of random complex samples, having amplitude equal to the square root of an exponentially-distributed variable with mean $S_x(f_k)$ and phase uniformly distributed in $[0, 2\pi]$, is inversely Fourier-transformed to yield the time-domain sequence $\{x_k\}$. Also other synthesis algorithms were essayed, with no substantially different results in comparing accuracies.

First, 100 independent pseudo-random sequences $\{x_k\}$ of length $N = 131072$, with mean $m_x=0$ and variance $\sigma_x^2=1$, were generated for each of the 11 values $\{H_i\} = \{0.50, 0.55, \dots, 1.00\}$, corresponding to $\{\alpha_i\} = \{0, -0.1, \dots, -1.0\}$. On the resulting 1100 time series, we applied the MHVAR-3, MAVAR and LD-3 methods, getting three sets of estimates $\{\hat{H}_{i,j}\}$, for $i = 0, 1, \dots, 10$ and $j = 1, 2, \dots, 100$. We then evaluated the accuracy of these estimates, calculating the absolute estimation errors $\Delta_{i,j} = \hat{H}_{i,j} - H_i$. Furthermore, we repeated the same test on another set of 1100 sequences of length $N = 1024$, to compare the methods on short sequences, where results are impaired by poor confidence.

Fig. 4 compares the estimation errors $\{\Delta_{i,j}\}$ attained by the three methods on sequences of $N = 131072$ samples. For each value H_i , the mean m_{Δ_i} and standard deviation $\pm\sigma_{\Delta_i}$, out of 100 estimation errors, are plotted. Both MAVAR and MHVAR-3 achieve better confidence (i.e., smaller σ_{Δ_i}) than LD-3 (cf. Fig. 8). Also, LD-3 estimates appear significantly biased.

Similarly, Fig. 5 compares the estimation errors $\{\Delta_{i,j}\}$ on sequences of $N = 1024$ samples. On short sequences, MHVAR-3 does not outperform MAVAR (cf. Fig. 8). Yet, both MAVAR and MHVAR-3 achieve much better confidence than LD-3, which seems less efficient on short data sequences.

Visual comparison of MAVAR/MHVAR and LD plots, not shown here for lack of space, justifies

such better confidence of H estimates. Especially on short sequences, MAVAR/MHVAR log-log plots are far smoother and closer to the ideal linear trend than LD, even at right where confidence is worse.

B. Impact of Steps Superposed to LRD Input Data

We evaluated MAVAR, MHVAR- M and LD-3 on LRD data with various steps superposed (cf. Sec. V.B). Sequences of length $N = 1024$ and $N = 131072$ were generated as $\{x_k\} = \{Au_{k-Q} + n_k\}$ ($k = 1, \dots, N$), where $\{u_{k-Q}\}$ is the sampled unit step function $u(t)$ delayed Q time units ($1 < Q < N$) and $\{n_k\}$ is a pseudo-random LRD series, with $m_n = 0$ and variance $\sigma_n^2 = 1$, generated as before with PSD $S_n(f) = hf^\alpha$ for $\alpha = -0.60$ ($H = 0.80$). By varying extensively parameters Q and A , we found that:

- ❑ the step impact on MHVAR- M is maximum for $Q \cong N/2$ and negligible for $Q \rightarrow 1$ and $Q \rightarrow N$;
- ❑ for M even, input steps affect MHVAR- M curves only at the right end;
- ❑ for M odd, input steps shift MHVAR- M curves vertically, with limited impact on their slope [49];
- ❑ the step size A must be at least on the order of σ_n to impact significantly MHVAR- M ; such big steps are evident by simple visual inspection and may be removed before H estimation, to avoid erroneous identification of random power-law noise;
- ❑ input steps affect MHVAR- M (M even) less than LD-3.

Among many simulation results, Figs. 6 and 7 show MAVAR and LD-3 curves for $N=131072$, varying step size and delay as $0 \leq A \leq 2$ and $0 < Q < N$. MHVAR- M curves for $M=3, 4$ (latter ones almost identical to that of MAVAR) are shown in [49]. To compare MHVAR and LD graphs fairly, note that MHVAR is plotted over the full range $n < N/(M+1)$, whereas LD omits the last two octaves ($j > 14$) [47].

C. Impact of the Difference Order M

We evaluated how the order M affects the MHVAR- M estimate accuracy, on 100 independent pseudo-random sequences $\{x_k\}$ of length N for each of the 11 values H_i as in Sec. VII.A. Fig. 8 plots, for $2 \leq M \leq 10$, the mean of the 11 mean values $m_{\Delta i}$ (dots) and of the 11 standard deviations $\sigma_{\Delta i}$ (bars) for $N = 1024$ (right) and $N = 131072$ (left). The LD-3 result is also plotted for comparison, although half out of scale.

First, MAVAR and MHVAR- M estimates appear not biased. Moreover, these results confirm the

1
2
3 better confidence of MHVAR-3 compared to MAVAR for $N=131072$: the mean of σ_{Δ_i} of MHVAR-3
4 estimates is -22% than that of MAVAR, which in turn is -14% than that of LD-3 (cf. Fig. 4). This
5 confidence gain is significant, since it is computed over 1100 independent estimates. For $N=1024$, the
6 mean of σ_{Δ_i} of MHVAR-3 estimates is just -3% than that of MAVAR, which is -54% than that of LD-3.
7
8

9
10
11 Conversely, we notice that increasing the order $M>4$ does not improve confidence further for
12 $N=131072$, whereas it even worsen it for $N=1024$. This behaviour on short series is explained considering
13 that estimator (12) averages less terms for larger M . In general, the confidence is not improved by
14 increasing the MHVAR order indefinitely, although $H_{MH}(f)$ becomes more selective (Fig. 2). Actually,
15 better spectral *resolution* does not mean more accurate estimation of the f^α spectrum slope, which decays
16 uniformly. Moreover, the sharper is the filter transfer function, the longer is its time-domain response, and
17 thus the longer the data sequence should be for achieving the same confidence.
18
19

20
21 Quite analogous considerations hold for the number of vanishing moments N_V in wavelet analysis.
22 As remarked in [8] by theoretical arguments, the larger N_V is, the better the H estimation by LD (smaller
23 bias and variance of the estimate). However, this improvement with increasing N_V is counterbalanced by
24 the increase of the number of wavelet coefficients polluted by border effects due to data finite length,
25 resulting in a smaller number of available wavelet coefficients and thus in a larger variance.
26
27

28 VIII. EXAMPLE OF APPLICATION TO A REAL IP TRAFFIC TRACE

29
30 We applied the MHVAR-3 and LD-3 methods on a real IP traffic series [bytes/s] measured on a
31 transoceanic link (MAWI [50]). This series is made of $N=61600$ samples, acquired with sampling period
32 $\tau_0=10$ ms over a measurement interval $T=616$ s. No nonstationary trends, such as steps, are evident.
33
34

35
36 Figs. 9 and 10 plot respectively LD-3 (1 point/octave) and MHVAR-3 (24 points/decade). We
37 notice that the LD-3 trend is more irregular (cf. Figs. 4 and 5), whereas MHVAR exhibits two regular
38 slopes, viz. $\mu_1 = -2.89$ and $\mu_2 = -1.8$. Almost no spurious ripples are visible.
39
40

41
42 Hence, two simple power-law (14) components are revealed by MHVAR: a main one with
43 $\alpha_1 \cong -0.11$ ($H \cong 0.555$), dominant for $10 \text{ ms} < \tau < 2 \text{ s}$, and a secondary one with $\alpha_2 = -1.2$, dominant for
44 $2 \text{ s} < \tau < 20 \text{ s}$. Both estimates are in agreement with average slopes observed on LD-3 [47] (note that
45
46
47
48
49
50
51
52
53
54
55
56
57
58
59
60

octave 8 corresponds to $\tau \cong 2$ s).

The different scaling behaviour exhibited by these traffic data on different observation intervals is somewhat common in experimental measurements [17]. In [3], such behaviour is referred to as *biscaling* phenomenon.

IX. CONCLUSIONS AND OPEN ISSUES FOR FURTHER STUDY

In this paper, the Modified Allan Variance and a Modified Hadamard Variance have been proposed for estimating the Hurst parameter H or the exponent α of traffic series with f^α power-law spectrum ($\alpha < 0$). MAVAR and MHVAR- M are kind of variances based on the second and M^{th} difference of input data, respectively. While MAVAR is widely used in frequency stability characterization and well studied in literature, MHVAR has been treated with little detail so far. In this work, properties of both variances were studied by analysis and simulation. Some other variances (e.g., total variances) were also studied, but resulted less interesting to the aim of H and α estimation.

The H estimation accuracy of MAVAR and MHVAR- M was evaluated on LRD pseudo-random sequences, generated with assigned values of H , and compared to the Daubechies' wavelet LD technique with 3 vanishing moments. Extensive simulations showed that MAVAR and MHVAR- M achieve significantly better confidence and are not biased in H estimation. On long sequences ($N=10^5$), the mean standard deviation of 1100 MHVAR-3 estimates resulted about 20% smaller than that of MAVAR, which in turn was about 15% smaller than that of LD-3. On short sequences ($N=10^3$), MHVAR-3 and MAVAR attained similar confidence, far better than LD-3 (mean deviation less than half). In general, increasing the order M may improve H estimation accuracy, but provided that the sequence is long enough, due to the larger number of samples involved in the variance definition.

The behaviour of MAVAR and MHVAR- M with drifts, steps and periodic components in input data was investigated. Being based on data M^{th} difference ($M \geq 2$), they cancel $\sim t^M$ drifts. Moreover, they proved quite robust against steps, being affected to a limited extent (or negligibly) and less than LD-3.

Finally, MHVAR-3 was computed on a real IP traffic trace. Compared to LD-3, MHVAR-3 gave a clearer spectral characterization of the traffic series analyzed. Two simple power-law noise components were identified, with PSD $k_1/f^{0.11} + k_2/f^{1.2}$, revealing different scaling behaviours dominant in different

observation intervals.

As far as the computational weight is concerned, MAVAR and LD have same complexity $O(N \log N)$, if MAVAR is computed by recursive algorithm for $n=2^j$, i.e. on octaves as LD.

In conclusion, MAVAR and MHVAR- M may complement usefully other well-established techniques (e.g. LD), due to several advantages. Among them, we highlight in particular:

- ❑ excellent spectral resolution (Figs. 2 and 3);
- ❑ efficient use of input data, yielding excellent accuracy and confidence in H and α estimation, with negligible bias (Figs. 4, 5 and 8); it is perhaps needless to remark that, if improving accuracy by few percentage points in estimating H and α may be considered of little practical interest, on the other hand more efficient tools allow to attain any desired accuracy requiring shorter data set;
- ❑ convergence to finite values for all types of f^α processes (14) with $\alpha > -1-2M$ ($\alpha \in \mathfrak{R}$);
- ❑ insensitivity to polynomial drifts of order up to $M-1$ and robustness against steps and periodic components, major examples of nonstationarity in traffic data;
- ❑ computational complexity affordable in all practical cases;
- ❑ ease of computation for *any* value of $\tau = n\tau_0$ ($n = 1, 2, \dots, \lfloor N/(M+1) \rfloor$), which allows rendering the trend to the finest detail (cf. LD, which is computed on octaves).

An important issue, still open for further study, is deriving analytical expressions for the confidence of H and α_i estimates by MAVAR/MHVAR and for their bias, if any. A possible approach may be to adapt the analysis carried out in [8], beginning with identifying appropriate wavelets for rephrasing definitions of MAVAR and MHVAR. More generally, further study is needed for providing a clearer picture of how MAVAR and MHVAR fit in the general framework of wavelet analysis.

REFERENCES

- [1] P. Abry, R. Baraniuk, P. Flandrin, R. Riedi, D. Veitch, "The Multiscale Nature of Network Traffic", *IEEE Signal Processing Mag.*, vol. 19, no. 3, pp. 28-46, May 2002.
- [2] K. Park, W. Willinger, "Self-Similar Network Traffic: An Overview", in *Self-Similar Network Traffic and Performance Evaluation*, K. Park, W. Willinger, Eds. Chichester, UK: John Wiley & Sons, 2000, pp. 1-38.
- [3] P. Abry, P. Flandrin, M. S. Taqqu, D. Veitch, "Wavelets for the Analysis, Estimation, and Synthesis of Scaling Data", in *Self-Similar Network Traffic and Performance Evaluation*, K.

- 1
2
3 Park, W. Willinger, Eds. Chichester, UK: John Wiley & Sons, 2000, pp. 39-88.
- 4
5 [4] V. Paxson, S. Floyd, "Wide-Area Traffic: the Failure of Poisson Modeling", *IEEE/ACM Trans.*
6 *Networking*, vol. 3, no. 6, pp. 226-244, June 1995.
- 7
8 [5] G. W. Wornell, A. V. Oppenheim, "Estimation of Fractal Signals from Noisy Measurements
9 Using Wavelets", *IEEE Trans. Signal Processing*, vol. 40, no. 3, pp. 611-623, March 1992.
- 10
11 [6] M. S. Taqqu, V. Teverovsky, W. Willinger, "Estimators for Long-Range Dependence: an
12 Empirical Study", *Fractals*, vol. 3, no.4, pp. 785-798, 1995.
- 13
14 [7] P. Abry, P. Gonçalvès, P. Flandrin, "Wavelets, Spectrum Analysis and $1/f$ Processes", in
15 *Lecture Notes in Statistics: Wavelets and Statistics*, vol 103, A. Antoniadis, G. Oppenheim,
16 Eds. Springer, 1995, pp. 15-29.
- 17
18 [8] P. Abry, D. Veitch, "Wavelet Analysis of Long-Range Dependent Traffic", *IEEE Trans. Inform.*
19 *Theory*, vol. 44, no.1, pp. 2-15, Jan. 1998.
- 20
21 [9] D. Veitch, P. Abry, "A Wavelet-Based Joint Estimator of the Parameters of Long-Range
22 Dependence", *IEEE Trans. Inform. Theory*, vol. 45, no.3, pp. 878-897, Apr. 1999.
- 23
24 [10] D. W. Allan, J. A. Barnes, "A Modified Allan Variance with Increased Oscillator
25 Characterization Ability", *Proc. 35th Annual Freq. Contr. Symp.*, 1981.
- 26
27 [11] P. Lesage, T. Ayi, "Characterization of Frequency Stability: Analysis of the Modified Allan
28 Variance and Properties of Its Estimate", *IEEE Trans. Instrum. Meas.*, vol. 33, no. 4, pp. 332-
29 336, Dec. 1984.
- 30
31 [12] L. G. Bernier, "Theoretical Analysis of the Modified Allan Variance", *Proc. 41st Annual Freq.*
32 *Contr. Symp.*, 1987.
- 33
34 [13] D. B. Sullivan, D. W. Allan, D. A. Howe, F. L. Walls, Eds., "*Characterization of Clocks and*
35 *Oscillators*", NIST Technical Note 1337, March 1990.
- 36
37 [14] S. Bregni, "Chapter 5 - Characterization and Modelling of Clocks", in *Synchronization of*
38 *Digital Telecommunications Networks*. Chichester, UK: John Wiley & Sons, 2002, pp. 203-
39 281.
- 40
41 [15] ITU-T Rec. G.810 "Definitions and Terminology for Synchronisation Networks", Rec. G.811
42 "Timing Characteristics of Primary Reference Clocks", Rec. G.812 "Timing Requirements of
43 Slave Clocks Suitable for Use as Node Clocks in Synchronization Networks", Rec. G.813
44 "Timing Characteristics of SDH Equipment Slave Clocks (SEC)", Geneva, 1996-2003.
- 45
46 [16] S. Bregni, L. Primerano, "The Modified Allan Variance as Time-Domain Analysis Tool for
47 Estimating the Hurst Parameter of Long-Range Dependent Traffic", *Proc. IEEE*
48 *GLOBECOM 2004*, Dallas, TX, USA, 2004.
- 49
50 [17] S. Bregni, W. Erangoli, "Fractional Noise in Experimental Measurements of IP Traffic in a
51 Metropolitan Area Network", *Proc. IEEE GLOBECOM 2005*, St. Louis, MO, USA, 2005.
- 52
53 [18] S. Bregni, R. Cioffi, M. Decina, "An Empirical Study on Statistical Properties of GSM
54 Telephone Call Arrivals", *Proc. IEEE GLOBECOM 2006*, S. Francisco, CA, USA, 2006.
- 55
56 [19] W. Vervaat, "Properties of General Self-Similar Processes", *Bulletin of the Internat. Statistical*
57 *Inst.*, vol. 52, pp. 199-216, 1987.
- 58
59 [20] P. Flandrin, "On the Spectrum of Fractional Brownian Motions", *IEEE Trans. Inform. Theory*,
60 vol. 35, no. 1, pp. 197-199, Jan. 1989.
- [21] J. Rutman, "Characterization of Phase and Frequency Instabilities in Precision Frequency Sources: Fifteen Years of Progress", *Proc. IEEE*, vol. 66, no. 9, pp. 1048-1075, Sept. 1978.
- [22] J. A. Barnes, A. R. Chi, L. S. Cutler, D. J. Healey, D. B. Leeson, T. E. McGunigal, J. A. Mullen Jr., W. L. Smith, R. L. Sydnor, R. F. C. Vessot, G. M. R. Winkler, "Characterization of Frequency Stability", *IEEE Trans. Instrum. Meas.*, vol. 20, no. 2, pp. 105-120, May 1971.

- [23] D. W. Allan, "Statistics of Atomic Frequency Standards", *Proc. IEEE*, vol. 54, no. 2, pp. 221-230, July 1966.
- [24] W. C. Lindsey, C. M. Chie, "Theory of Oscillator Instability Based upon Structure Functions", *Proc. IEEE*, vol. 64, no. 12, pp. 1652-1666, Dec. 1976.
- [25] L. S. Cutler, C. L. Searle, "Some Aspects of the Theory and Measurement of Frequency Fluctuations in Frequency Standards", *Proc. IEEE*, vol. 54, no. 2, pp. 136-154, Feb. 1966.
- [26] P. Lesage, C. Audoin, "Characterization and Measurement of Time and Frequency Stability", *Radio Science (American Geophysical Union)*, vol. 14, no. 4, pp. 521-539, 1979.
- [27] F. L. Walls, D. W. Allan, "Measurement of Frequency Stability", *Proc. IEEE*, vol. 74, no. 1, pp. 162-168, Jan. 1986.
- [28] J. Rutman, F. L. Walls, "Characterization of Frequency Stability in Precision Frequency Sources", *Proc. IEEE*, vol. 79, no. 6, pp. 952-960, June 1991.
- [29] J.-F. Coeurjolly, "Simulation and Identification of the Fractional Brownian Motion: a Bibliographical and Comparative Study", *J. of Stat. Software*, vol. 5, no. 7, 2000, pp. 1-53.
- [30] J.-F. Coeurjolly, "Estimating the Parameters of a Fractional Brownian Motion by Discrete Variations of Its Sample Paths", *Stat. Inference Stoch. Process*, Kluwer Academic Publishers, vol. 4, no. 2, 2001, pp. 199-227.
- [31] P. Lesage, C. Audoin, "Characterization of Frequency Stability: Uncertainty Due to the Finite Number of Measurements", *IEEE Trans. Instrum. Meas.*, vol. 22, no. 2, pp. 157-161, June 1973. "Comments on '—'", *IEEE Trans. Instrum. Meas.*, vol. 24, no. 1, p. 86, Mar. 1975. "Correction to '—'", *IEEE Trans. Instrum. Meas.*, vol. 25, no. 3, p. 270, Sept. 1976.
- [32] P. Lesage, C. Audoin, "Estimation of The Two-Sample Variance with Limited Number of Data", *Proc. 31st Annual Freq. Contr. Symp.*, 1977.
- [33] K. Yoshimura, "Characterization of Frequency Stability: Uncertainty Due to the Autocorrelation Function of Frequency Fluctuations", *IEEE Trans. Instrum. Meas.*, vol. 27, no. 1, pp. 1-7, Mar. 1978.
- [34] S. R. Stein, "Frequency and Time - Their Measurement and Characterization", in *Precision Frequency Control*, vol. 2, ch. 2, E. A. Gerber A. Ballato, Eds. New York: Academic Press, 1985, pp. 191-232.
- [35] C. A. Greenhall, "Recipes for Degrees of Freedom of Frequency Stability Estimators", *IEEE Trans. Instrum. Meas.*, vol. 40, no. 6, pp. 994-999, Dec. 1991.
- [36] C. A. Greenhall, W. J. Riley. "Uncertainty of Stability Variances Based on Finite Differences". Available: <http://www.wiley.com>.
- [37] W. J. Riley, "Confidence Intervals and Bias Corrections for the Stable Variance Functions", Hamilton Technical Services, 2000. Available: <http://www.wiley.com>.
- [38] D. W. Allan, M. A. Weiss, J. L. Jespersen, "A Frequency-Domain View of Time-Domain Characterization of Clocks and Time and Frequency Distribution Systems", *Proc. 45th Annual Freq. Contr. Symp.*, 1991.
- [39] C. A. Greenhall, D. A. Howe, D. B. Percival, "Total Variance, an Estimator of Long-Term Frequency Stability", *IEEE Trans. Ultrason., Ferroelect., Freq. Contr.*, vol. 46, no. 5, pp. 1183-1191, Sept. 1999.
- [40] D. A. Howe, "Total Variance Explained", *Proc. 1999 Joint Meeting of the European Freq. and Time Forum and the IEEE Int. Freq. Contr. Symp.*, pp. 1093-1099, April 1999.
- [41] D. A. Howe, "The Total Deviation Approach to Long-Term Characterization of Frequency Stability", *IEEE Trans. Ultrason., Ferroelect., Freq. Contr.*, vol. 47, no. 5, pp. 1102-1110, Sept. 2000.
- [42] D. A. Howe, T. K. Pepler, "Definitions of 'Total' Estimators of Common Time-Domain

- 1
2
3 Variances", *Proc. 2001 IEEE Int. Freq. Contr. Symp.*, pp. 127-132, June 2001.
- 4
5 [43] R. A. Baugh, "Frequency Modulation Analysis with the Hadamard Variance", *Proc. 25th*
6 *Annual Freq. Contr. Symp.*, pp. 222-225, Apr. 1971.
- 7
8 [44] W. J. Riley, "The Hadamard Variance", Hamilton Technical Services, 1999. Available:
9 <http://www.wiley.com>.
- 10
11 [45] D. A. Howe, R. Beard, C. A. Greenhall, F. Vernotte, W. J. Riley, "A Total Estimator of the
12 Hadamard Function Used for GPS Operations", *Proc. 32nd PTI Meeting*, Nov. 2000.
- 13
14 [46] F. Vernotte, G. Zalamansky, M. Mc Hugh, E. Lantz, "Estimation of the Upper Limit on the
15 Level of an Undetected Noise - Application to the Study of Millisecond Pulsars", *Proc. 1996*
16 *IEEE Int. Freq. Contr. Symp.*, pp. 875-879, June 1996.
- 17
18 [47] D. Veitch. "Code for The Estimation of Scaling Exponents". Available:
19 http://www.cubinlab.ee.mu.oz.au/~darryl/secondorder_code.html.
- 20
21 [48] V. Paxson, "Fast Approximation of Self-Similar Network Traffic", *ACM/SIGCOMM Computer*
22 *Communication Review*, vol. 27, no. 7, pp. 5-18, Oct. 1997.
- 23
24 [49] S. Bregni, L. Jmoda, "Improved Estimation of the Hurst Parameter of Long-Range
25 Dependent Traffic Using the Modified Hadamard Variance", *Proc. IEEE ICC 2006*, Istanbul,
26 Turkey, 2006.
- 27
28 [50] MAWI (Measurement and Analysis on the WIDE Internet). Trace: 25 Jan 2005, 14:00.
29 Available: <http://tracer.csl.sony.co.jp/mawi/>
- 30
31
32
33
34
35
36
37
38
39
40
41
42
43
44
45
46
47
48
49
50
51
52
53
54
55
56
57
58
59
60

FIGURES

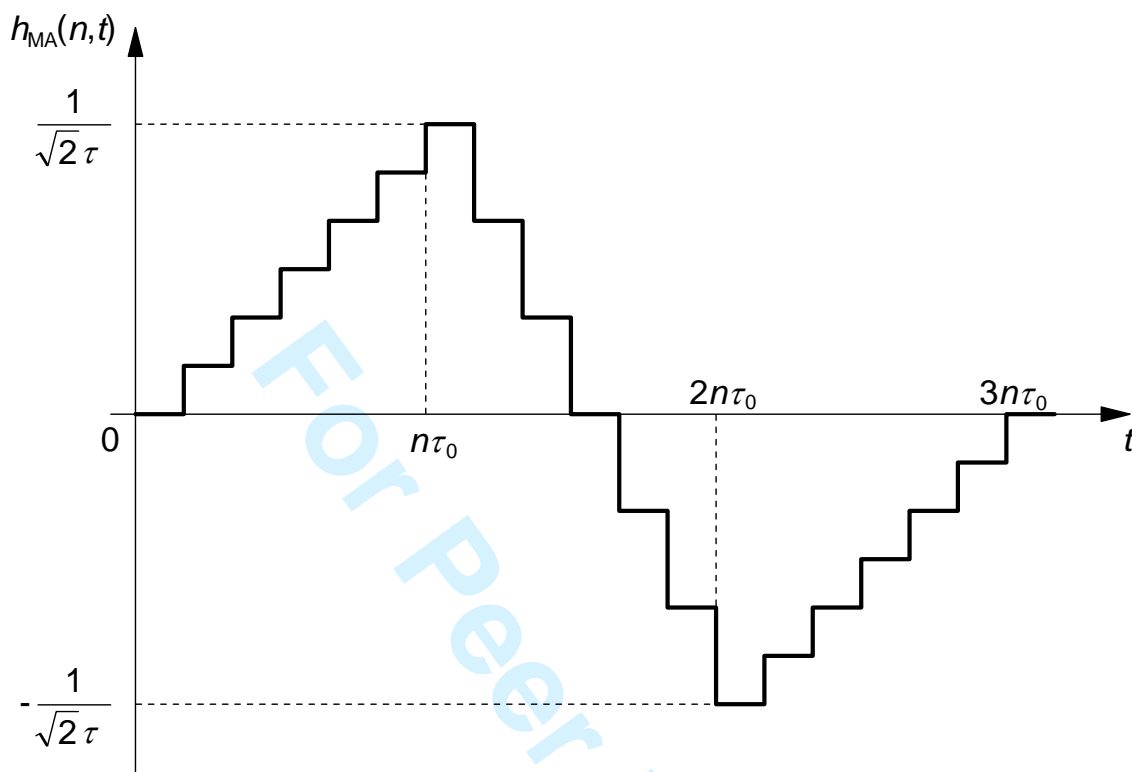


Fig. 1: Impulse response of the filter associated to the definition of MAVAR ($n=6$).

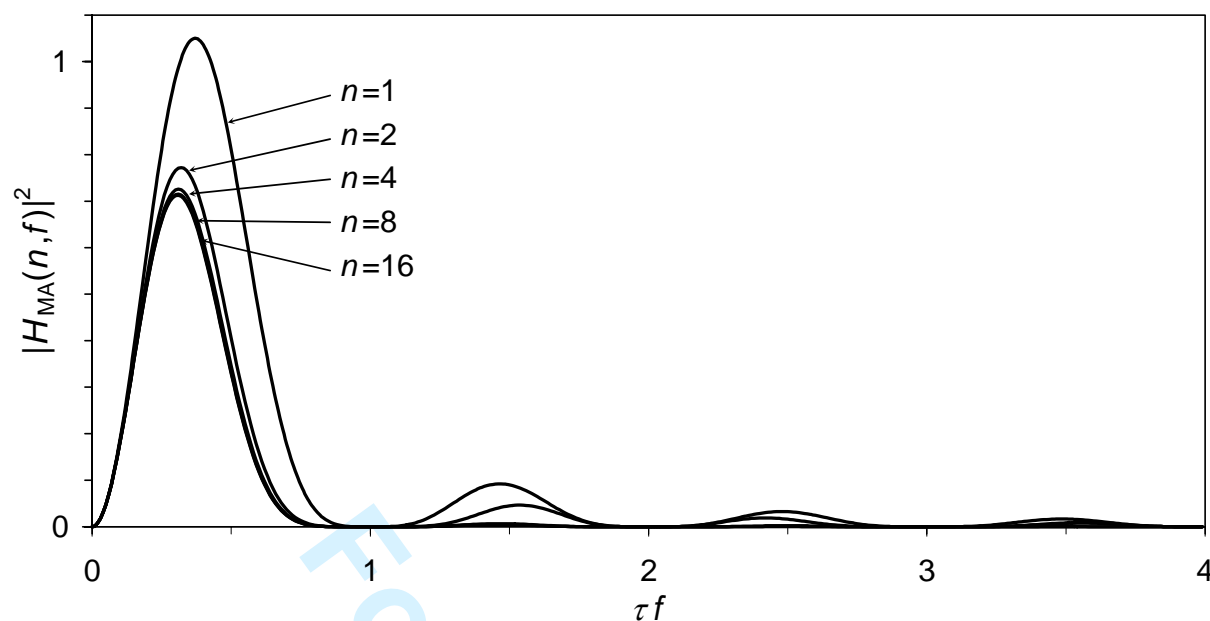


Fig. 2: Square magnitude of the MAVAR transfer function for various values of n .

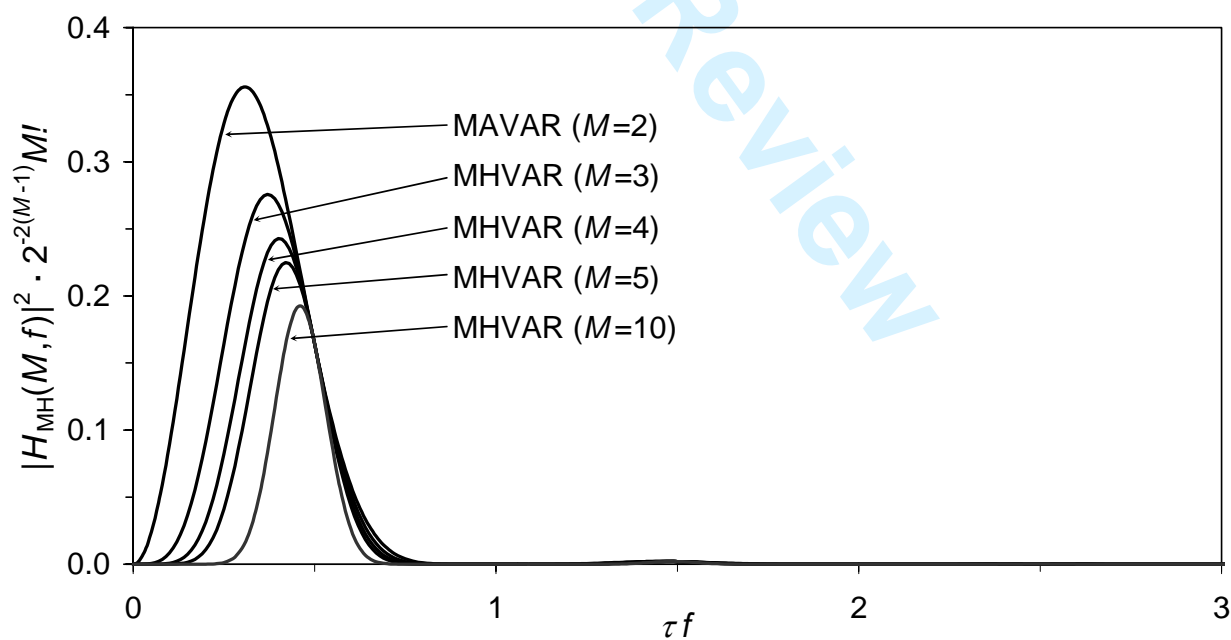


Fig. 3: Normalized square magnitude of MHVAR- M asymptotic transfer functions.

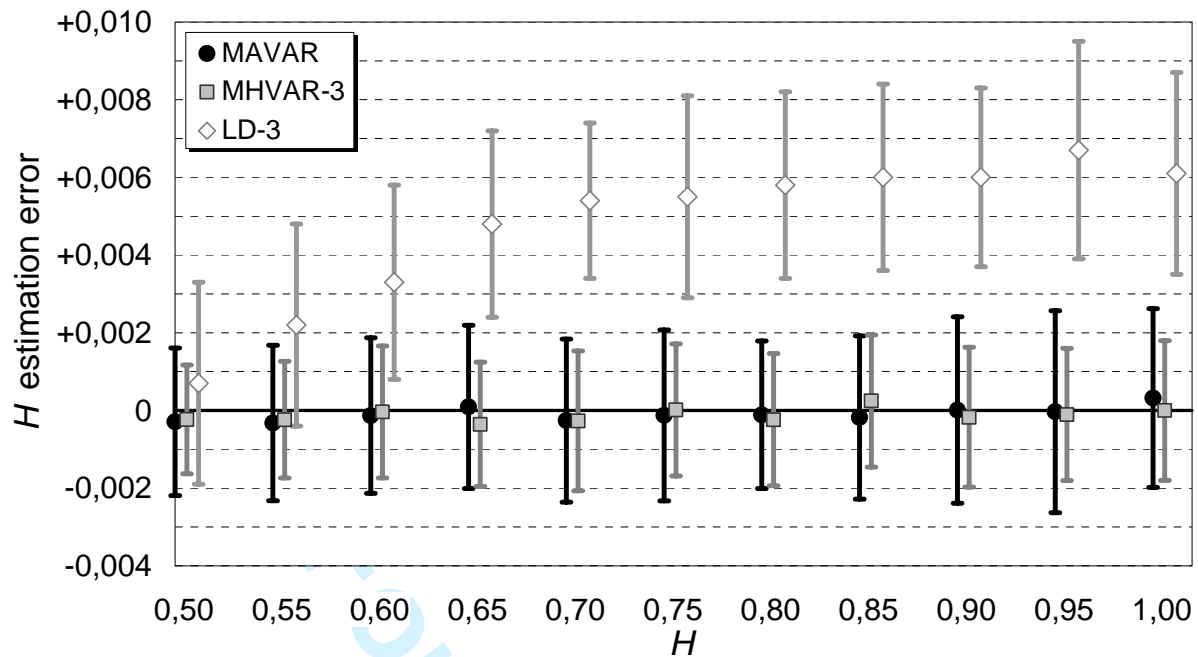


Fig. 4: Absolute estimation error of H attained by MAVAR, MHVAR-3 and LD-3 methods ($N=131072$, mean and standard deviation out of 100 estimation errors).

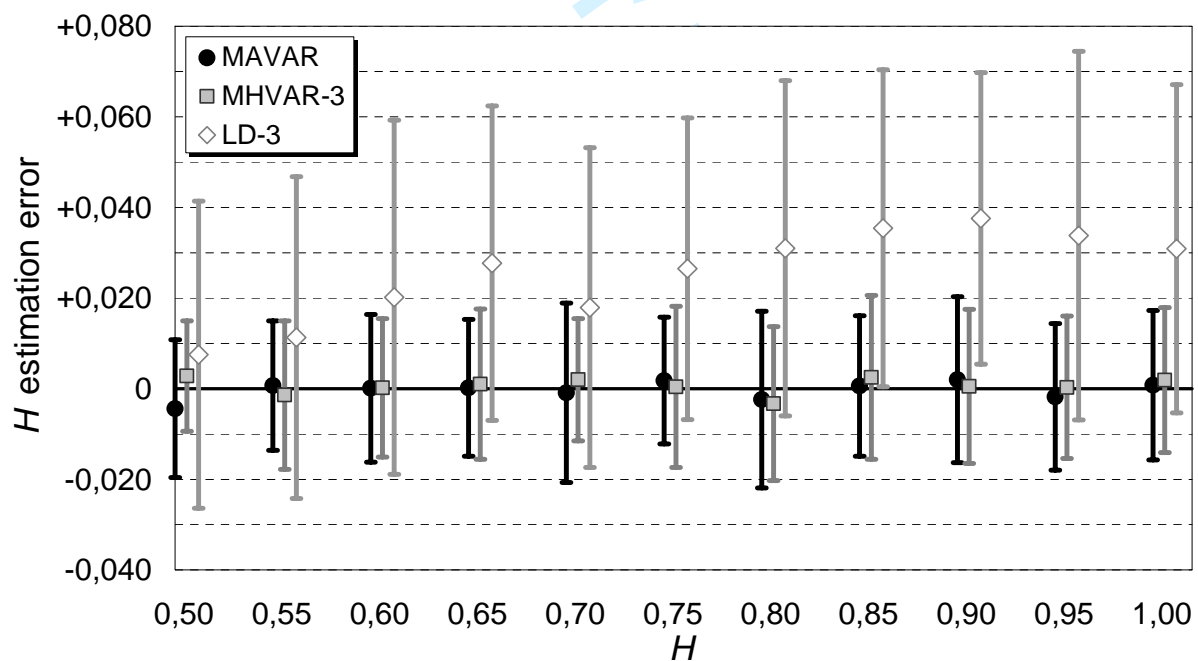


Fig. 5: Absolute estimation error of H attained by MAVAR, MHVAR-3 and LD-3 methods ($N=1024$, mean and standard deviation out of 100 estimation errors).

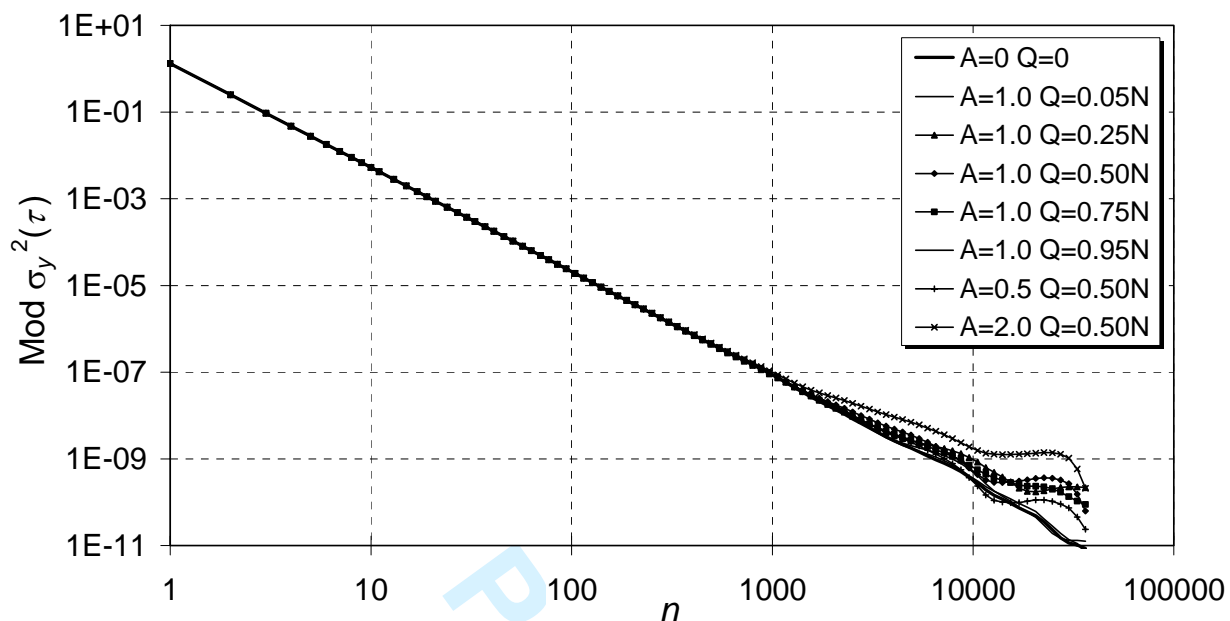


Fig. 6: MAVAR computed on a pseudo-random LRD sequence $\{n_k\}$ ($N=131072$, $m_n=0$, $\sigma_n=1$, $H=0.80$) with added step $\{Au_{k,0}\}$.

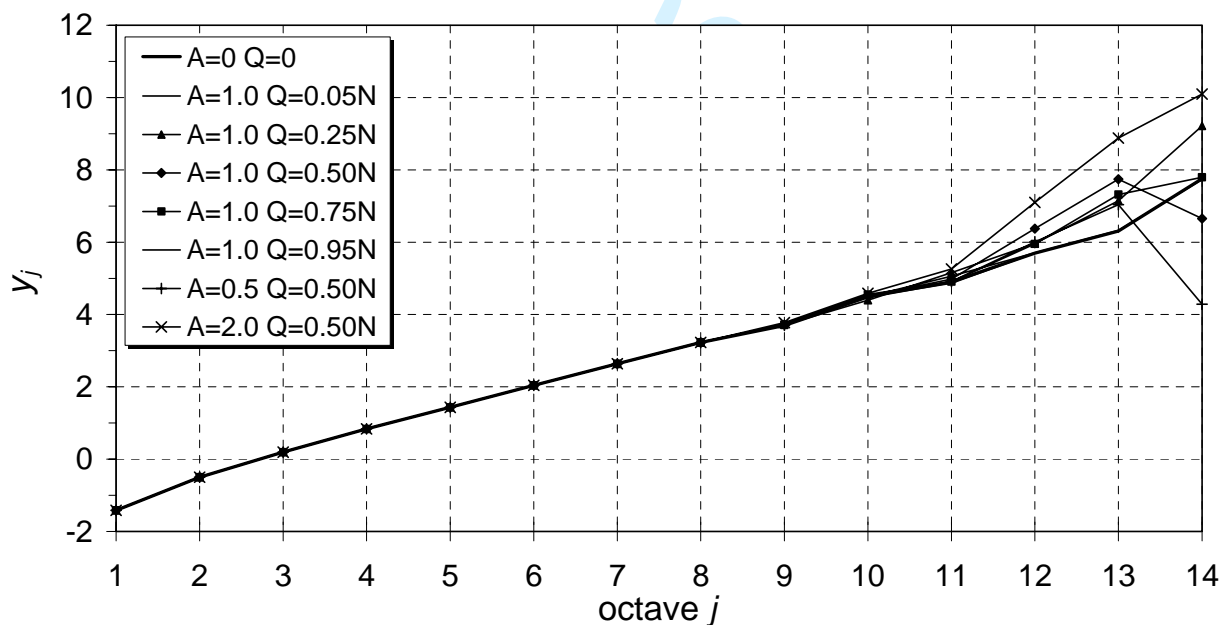


Fig. 7: LD-3 computed on a pseudo-random LRD sequence $\{n_k\}$ ($N=131072$, $m_n=0$, $\sigma_n=1$, $H=0.80$) with added step $\{Au_{k,0}\}$.

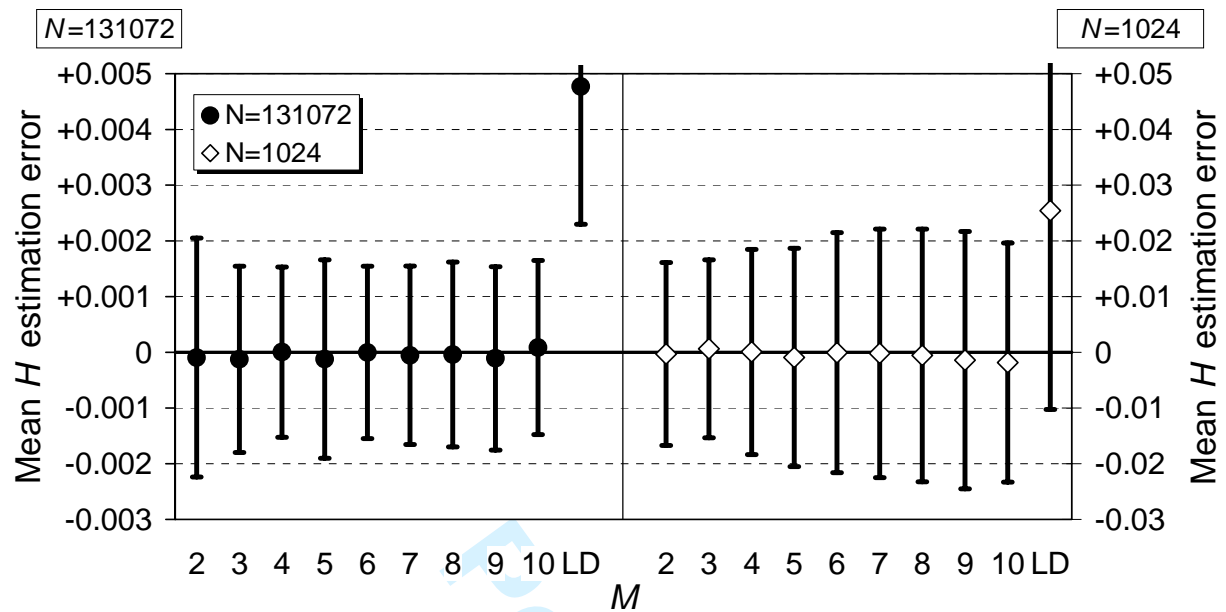


Fig. 8: Average mean $E[m_{\Delta_i}]$ and standard deviation $E[\sigma_{\Delta_i}]$ ($i = 0, \dots, 10$) of the H estimation errors attained by the MHVAR- M method ($2 \leq M \leq 10$), compared to LD-3 (average results on 100 pseudo-random sequences $\{x_k\}$ for each of 11 values H).

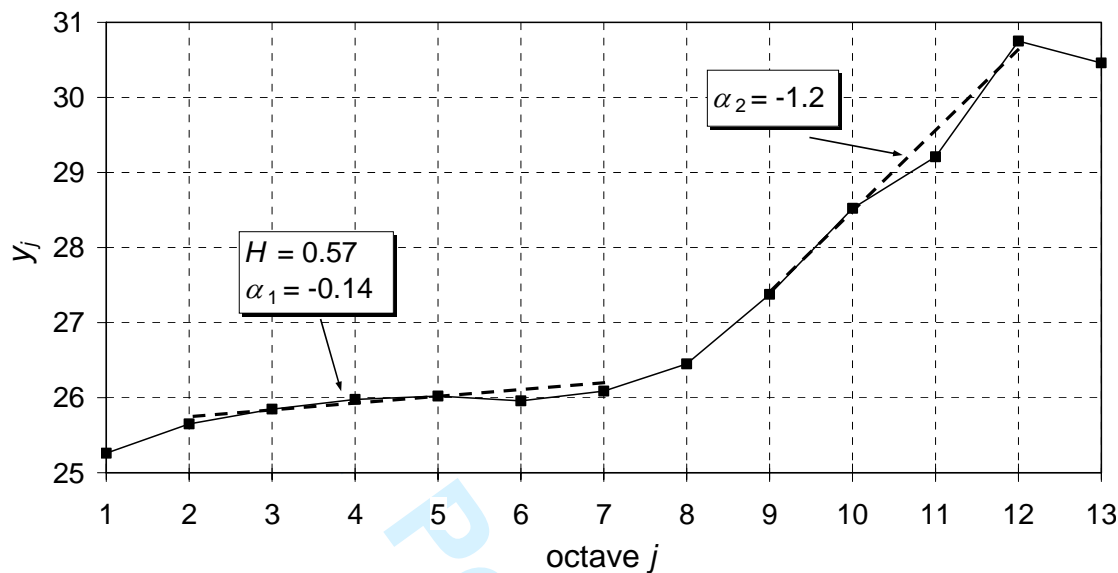


Fig. 9: Logscale diagram (3 vanishing moments) [47] of a real IP bytes/time trace (MAWI Project [50], $N=61600$, $\tau_0=10$ ms, $T=616$ s).

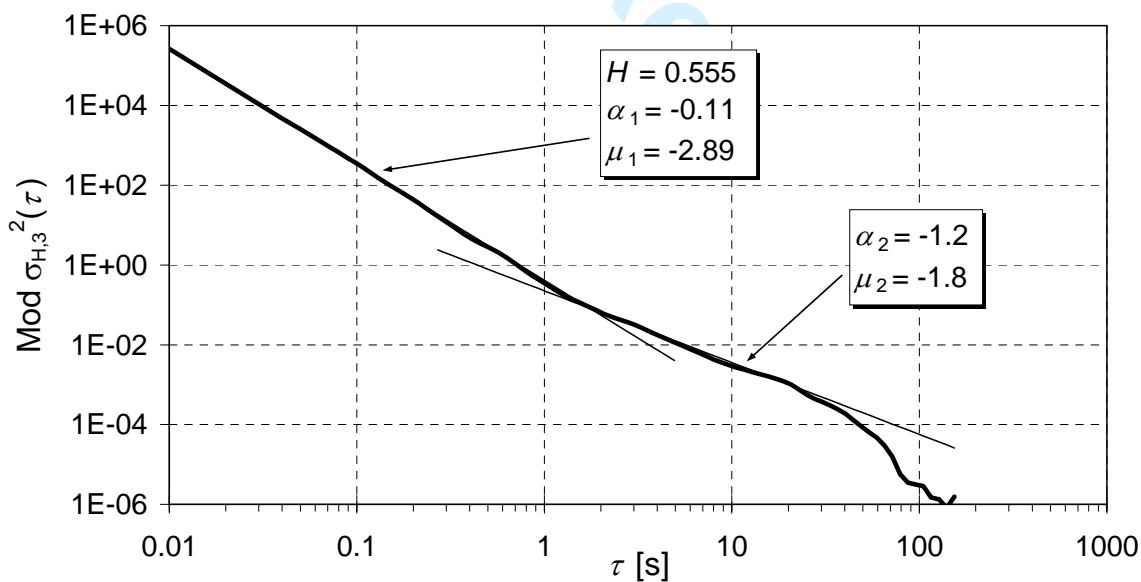


Fig. 10: Modified Hadamard Variance ($M=3$) of a real IP bytes/time trace (MAWI Project [50], $N=61600$, $\tau_0=10$ ms, $T=616$ s).